Effects of Periodic Charge Boundary Conditions on the Poisson Boltzmann Equation

Sernyik Raymen Chee
MIT ID: 927706156
Course 8.592
Statistical Physics in Biology
Massachusetts Institute of Technology
Cambridge, MA 02139
USA

Submitted to
Professor Mehran Kardar
&
Professor Leonid Mirny

May 12, 2005

e-mail address: raymen@mit.edu

Effects of Periodic Charge Boundary Condition on the Poisson Boltzmann Equation

Abstract

In this paper, the behavior of 1:1 electrolytes in the presence of charge fluctuations at the boundaries is investigated by solving the 2-D Poisson Boltzmann equation in rectangular geometry. The partial differential equation is first solved numerically before various perturbative approximations that expand around the exact 1-D solution is proposed and shown to be in good agreement with numerical results. It is found from both approximate and exact results that electrolytes feel less of the charge fluctuations as the magnitude of the charge density at the boundary increases. It is also observed that the ratio of the screening length to the logarithm of wavelength of the charge fluctuations can be related to the charge densities exponentially. Unfortunately, none of the approximate solutions are unable to capture this behavior.

1. Introduction

To model the electrostatic properties of biological systems, like proteins and DNA in a sea of electrolytes, the Poisson Boltzmann equation is often used as a starting point to calculate potential and charge distributions. In fact, the behavior of electrolytes near a charged interface has also been of great interest to chemists and physicists in last century. For instance, the standard Debye-Huckel theory [1,2] is a weak linearization of the Poisson Boltzman equation. Lars Onsager's [3] modification of Poisson Boltzmann equation with the incorporation of image forces enjoyed great success at low electrolyte concentrations. There have also been many attempts to extend the theory to higher concentrations. These attempts often involve the use of more advanced statistical mechanics methods, like integral equations [4-7] and density functional theory [8-13]. More recently, Netz et al [14-17] applied field theoretic methods to capture the fluctuation effects and correlation functions of charged systems where the Poisson Boltzmann equation is obtained as a saddle point of the field theoretic action. Unfortunately, all these methods provide little success in reproducing the results obtained from molecular dynamics [18] and Monte Carlo simulations. In a numerical study, Bhatt et al [19] suggested the failure is due to the dielectric continuum approximation of water.

Without explicit water molecules, it is impossible to ever capture the importance of ion-water correlations at high salt concentrations.

Surprisingly, there has been little literature in the theoretical study of 2-D Poisson Boltzmann equations and the effects of periodically distributed charges at the interface. Most of the systems solved in literature are averaged out in space and account for 1-D systems only. In this paper, the study of the 2-D electrostatic potential near a periodically charged plate via the Poisson Boltzmann equation will be provided. The study will comprise of three parts. In the first part, the numerical solution will be compared to both perturbative and linearised solutions of the 2-D Poisson Boltzmann equation. In the second part, the variation in the screening of electrolytes from the surface charge distribution and its dependence on the magnitude of the surface charge will be investigated. In the last part, the significance of long and short wavelength charge distributions at the boundaries will be quantified.

2. Model

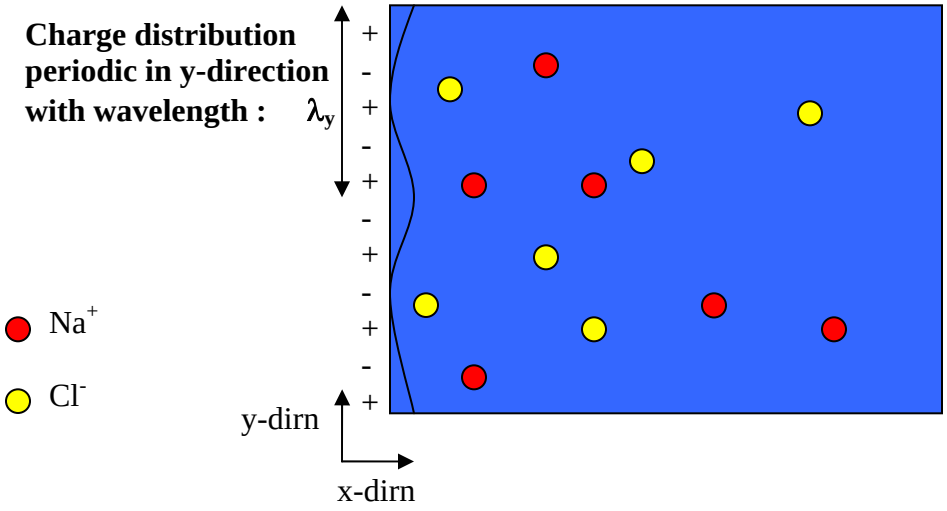

Figure 1: Diagram of periodically charged plate in a sea of +ve and –ve ions

The diagram above illustrates the system of interest in this study. There are two different ions present in the solution, i.e Na^+ and Cl^-. In the Poisson Boltzmann approach, they are modeled as point charges which do not interact with each other directly. They

feel the charges at the interface and being in a dielectric water medium. The positive and negative ions interact indirectly through screening. The charge at the plate is periodic in the y-direction and extends infinitely in the y and z-direction. The differential equation to be solved is given below:

$$\frac{\partial^2\phi}{\partial x^2}+\frac{\partial^2\phi}{\partial y^2}=-\sum_{i=1}^{2}\frac{\rho_{i,\infty}z_i e}{\varepsilon}\exp\left[\frac{-z_i e\phi(x,y)}{kT}\right] \quad \textit{2 - D Poisson Boltzmann Equation}$$

$$\left.\frac{\partial\phi}{\partial x}\right|_{x=0}=\frac{-\sigma}{2\varepsilon}\left[1+\eta\cos\left(\frac{y}{\lambda_y}\right)\right] \quad \& \quad \phi=\left.\frac{\partial\phi}{\partial x}\right|_{x=\infty}=0 \;\; \textit{Charge conditions}$$

$$\left.\frac{\partial\phi}{\partial y}\right|_{y=0}=\left.\frac{\partial\phi}{\partial y}\right|_{y=\lambda_y}=0 \qquad \textit{Periodic Boundary Conditions}$$

To solve the non-linear PDE, the finite difference method is used to discretize the equation into a set of 600 x-variables by 50 y-variables algebraic equations. Fortunately, the Jacobian of the set of non-linear algebraic equations can be computed analytically and much time is saved in inverting the sparse 30000 by 30000 matrix in Matlab. Conservation of charges is used to as a criteria to validate the numerical code.

3. Approximate analytical forms of the solution

a. Perturbative Approach

It is desired to obtain an approximate form of solution for the 2-D Poisson Boltzmann equation. An analytical form of the solution can often provide more insight than the exact numerical results.

First it is important to note that the PDE we are solving is in principle semi-2D. The infinite and periodic nature of the charge distribution in y implies that the length scale in the y-direction, λ_y is fixed. When the ratio of the length scale in the x and y direction is small, it should be possible to expand the solution around the 1-D Poisson Boltzmann equation. By defining the Debye length to be $\lambda_x=\sqrt{kT\varepsilon/z^2e^2\rho_\infty}$, $\psi=ze\phi/kT$ and $X=\frac{x}{\lambda_x}$ and $Y=\frac{y}{\lambda_y}$, the parameter, κ arises from non-dimensionalising the 2D Poisson Boltzmann equation:

$$\frac{\partial^2\psi}{\partial X^2}+\kappa\frac{\partial^2\psi}{\partial Y^2}=2\sinh(\psi)\ where\ \kappa=\left(\frac{\lambda_x}{\lambda_y}\right)^2$$ ---------- eqn (1)

By assuming that ψ can be expanded as $\psi_o(x)+\kappa\psi_1(x,y)+\kappa^2\psi_2(x,y)+\ldots$, and taking non-linearities to be dominant in the x direction since κ is small, equation 1 can be rewritten as a series of ordinary differential equations. The series of equations are given as follows:

$$\frac{\partial^2\psi_0}{\partial X^2}=2\sinh(\psi_o) \qquad \text{and} \qquad \frac{\partial^2\psi_2}{\partial X^2}+\frac{\partial^2\psi_1}{\partial Y^2}=2\sinh(\psi_o)\psi_2$$

$$\frac{\partial^2\psi_1}{\partial X^2}=2\cosh(\psi_o)[\psi_1]$$

The beauty of this expansion is that an analytical form of the solution for ψ_o is available. An analytical series expansion for the solution for ψ_1 can subsequently be obtained. However, ψ_2 must be solved numerically. Interestingly, the expansion of the solution to the order in κ is enough to capture most of the effects of the periodic charge distribution. Incorporation of the equations second order in κ actually leads to over correction and oscillations in the x direction not observed in the numerical results and will be neglected in this paper.

The details of the math can be found in appendix A. The full solution to the first order in κ is also given in appendix A. An approximate solution for analysis purposes is given below:

$$\psi_{per}=2\ln\left(\frac{1+A\exp\left(-\sqrt{2}X\right)}{1-A\exp\left(-\sqrt{2}X\right)}\right)-\frac{\lambda_x e\sigma}{\sqrt{2}\varepsilon kT}\eta\cos(Y)\frac{1}{A^2}\left[\frac{\left(1-A^2\exp\left(-\sqrt{2}X\right)\right)^{(1+\sqrt{3})/2}-\left(1-A^2\exp\left(-\sqrt{2}X\right)\right)^{(1-\sqrt{3})/2}}{\left(1+\sqrt{3}\right)\left(1-A^2\right)^{(-1+\sqrt{3})/2}-\left(1-\sqrt{3}\right)\left(1-A^2\right)^{-(1+\sqrt{3})/2}}\right]$$

$$A=\frac{2}{\sigma}\left[\sqrt{\sigma^2+8\rho kT\varepsilon}-\sqrt{8\rho kT\varepsilon}\right]---------- Eqn\ (2)$$

b. Linearized Solution

Alternatively, for small surface charge(<0.1Cm^{-2}) and low salt concentration(i.e. <1 M), the 2D Poisson Boltzmann equation can be linearized and solved analytically using eigenfunction expansion. This is a standard technique used in solving transport and diffusion problems and can be found in [20]. The linearized form of the Poisson

Boltzmann equation is analogous to the Debye Huckel theory for the 1-dimensional case. Details are provided in appendix A. The solution is given as follows:

$$\psi_{linear} = \frac{-\lambda_x e\sigma}{2\sqrt{2}\varepsilon kT}\left[\exp\left(-\sqrt{2}X\right)+\frac{\eta\cos(Y)}{\sqrt{2\pi^2+1}}\exp\left(-\sqrt{2+4\pi^2}X\right)\right] \quad \text{----------eqn (3)}$$

c. Naïve Form of Solution

Finally, the last and most naïve approach to obtain an approximate solution to the 2-D Poisson Boltzmann equation is by solving the problem exactly in 1-D and incorporate the y-dependence of the potential through the boundary conditions. The solution is therefore very similar to the perturbative case except for the y dependence in A. The solution is given in the expressions below:

$$\psi_{naive} = 2\ln\left(\frac{1+A(Y)\exp\left(-\sqrt{2}X\right)}{1-A(Y)\exp\left(-\sqrt{2}X\right)}\right)$$

$$A(Y) = \frac{2}{\sigma(y)}\left[\sqrt{\sigma(y)^2+8\rho kT\varepsilon}-\sqrt{8\rho kT\varepsilon}\right] \quad \text{----------eqn (4)}$$

$$\sigma(y) = \sigma_o\left[1+\eta\cos(Y)\right]$$

It turns out that this method provides the best estimates of how the electrostatic potential changes near the charged interface. Unfortunately, as shown later, it is unable to account for the correlation between that of the screening length and the wavelength of the charge distribution.

d. Comparison to Numerical Calculations.

Before examining the effects of the periodic charge distribution, it is instructive to see how the solutions of the different approximations compare to the actual numerical results and perhaps draw some conclusions about the region where non-linearity are the most important.

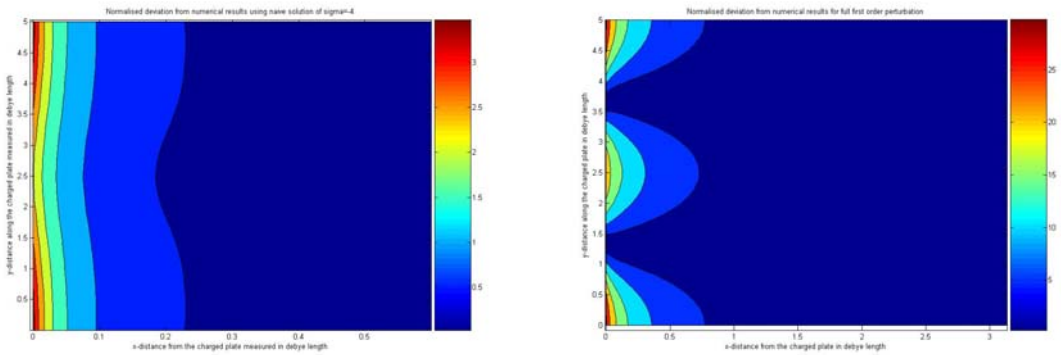

Figure 2: Contour plot of deviation of naïve and perturbative approximations from numerical result at σ=-4 Cm^{-2}. Note the difference in the length scale of variations.

From the contour plots above, it is clear that at high surface charge, the naïve approximation of the solution is much better and deviates slightly from the numerical solution. However this is not true when one looks at the contour plot at low surface charge i.e σ=-0.1 Cm^{-2}. To better illustrate the differences in the results obtained from the different approximations, the middle of the charged plate (i.e. Y=0.5) where there is greatest variation is plotted. Cross sectional plots of how the approximations compare with numerical results at different surface charges are shown in the figures below:

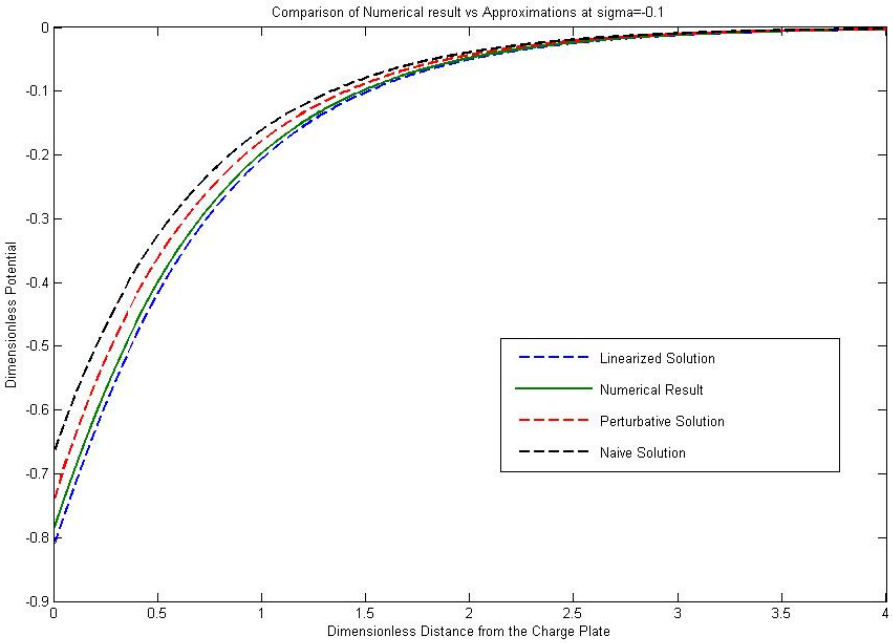

Figure 3: Comparison of approximations to numerical results for σ=-0.1.

Note how well the linear solution predicts the electrostatic potential.

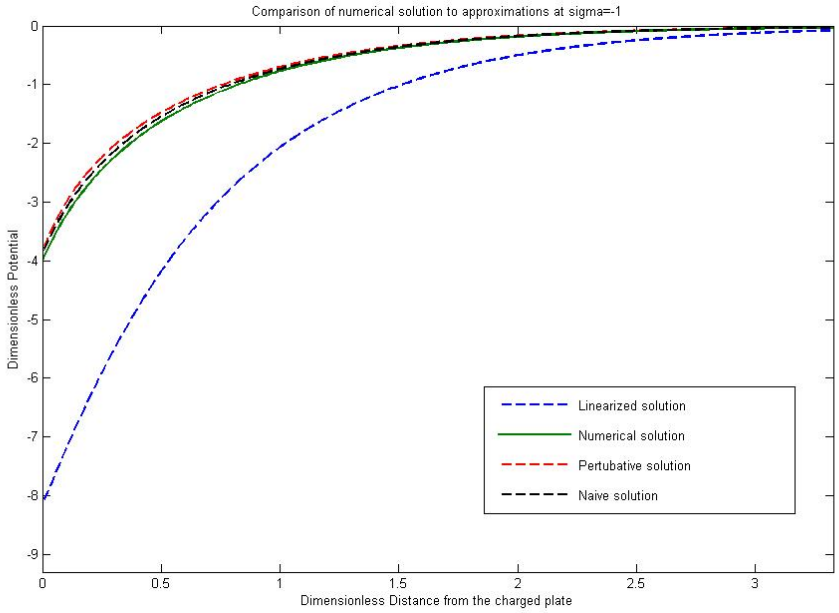

Figure 4: Comparison of approximations to numerical results for σ=-1

Note the breakdown of the linear solution.

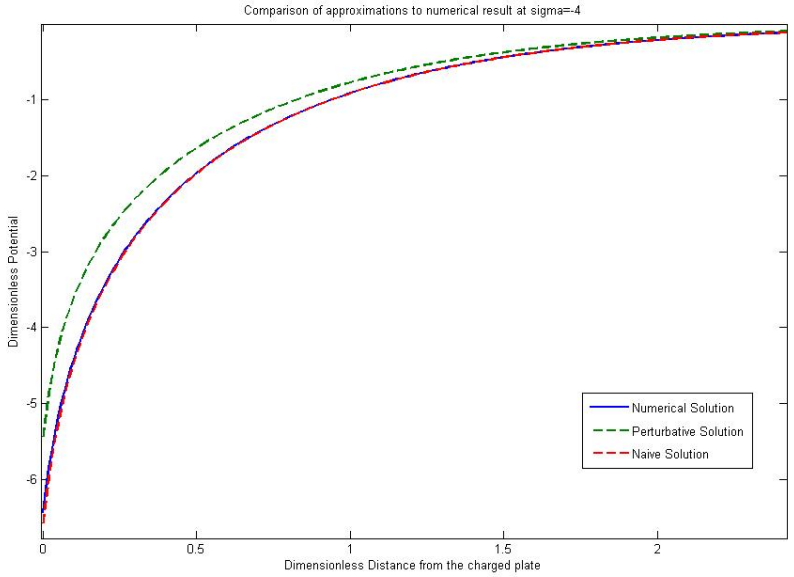

Figure 5: Comparison of approximations to numerical results for σ=-4

From the figures above, it is obvious that linearized form of the solution breakdowns rapidly even for moderate charges of -1.0 Cm^{-2} and can therefore not be used to study effects of the periodic charge distribution.

Another important observation is that as surface charge density increases, fluctuations in the y-direction becomes relatively unimportant compared to the x-direction. This in turn validates the perturbative and naive approximations and results in a better agreement with the numerical solution.

4. Effects of periodic charge distribution at the surface

With a better understanding of the validity of the different approximations, we are now equipped to study the effects arising from the periodicity in charge distribution. In particular, it is desired to quantify how the screening length changes as a function of surface charge density. (i.e. the minimum distance from the charge plate where the effect of fluctuating charge distribution is unfelt)

First, the parameter, χ in equation 5 is used to measure the deviation of the inhomogeneous electrostatic potential from the homogeneous electrostatic potential. There are two reasons for normalizing the variation with the potential at the homogeneous charged surface. Firstly, far away from the plate where ψ is close to zero, this definition prevents us from dividing by zero. Secondly, it is necessary to properly normalize χ in order to compare the results from different surface charge conditions.

$$\chi(X,Y) = \left| \frac{\psi_{in\,\mathrm{hom}\,ogenous} - \psi_{\mathrm{hom}\,ogenous}}{\psi_{\mathrm{hom}\,ogenoue,x=0}} \right| \times 100\% \quad \text{----------eqn(5)}$$

It is observed that deviations are most long lived near the “center” of the plate. Therefore, the screening length, L_x has been defined to be the length scale in the x-direction that satisfies the following equation:

$$\chi(L_x, 0.5) = 1 \quad \text{----------eqn(6)}$$

The contour plots of χ at which $\lambda_y = 5\lambda_x$, for different charge densities σ are given in figures 6-8 on the next page.

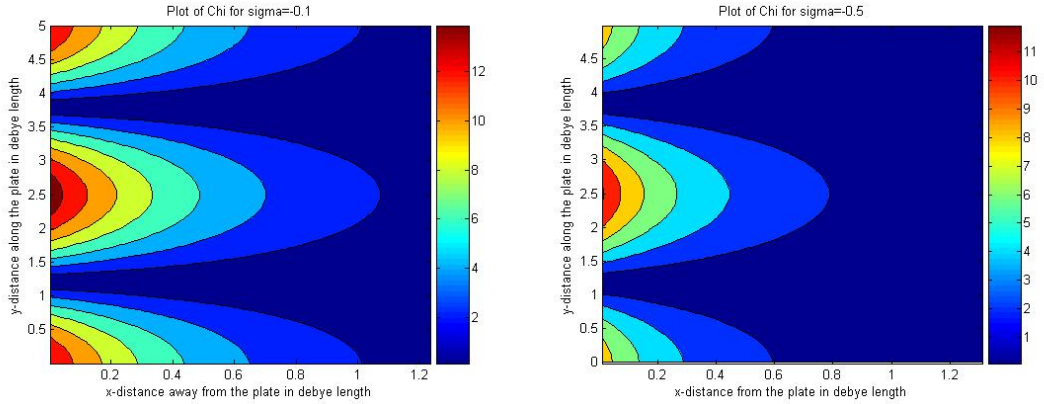

Figure 6: Plot of χ at low surface charge densities. Note how the screening length extends to over 1 debye length

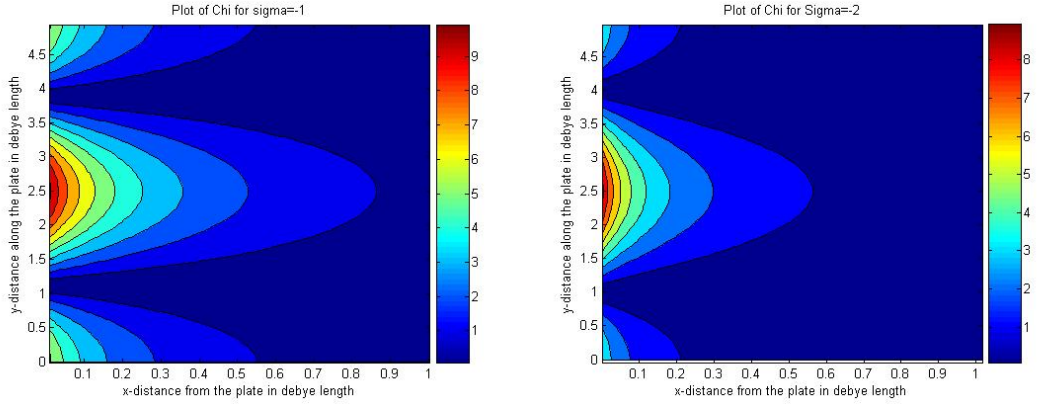

Figure 7: Plot of χ at moderate surface charge densities. Note how the screening length decreases as a surface charge density increases. Note also how variations near Y=0 and Y=λ_y diminishes in importance as surface charge density increases.

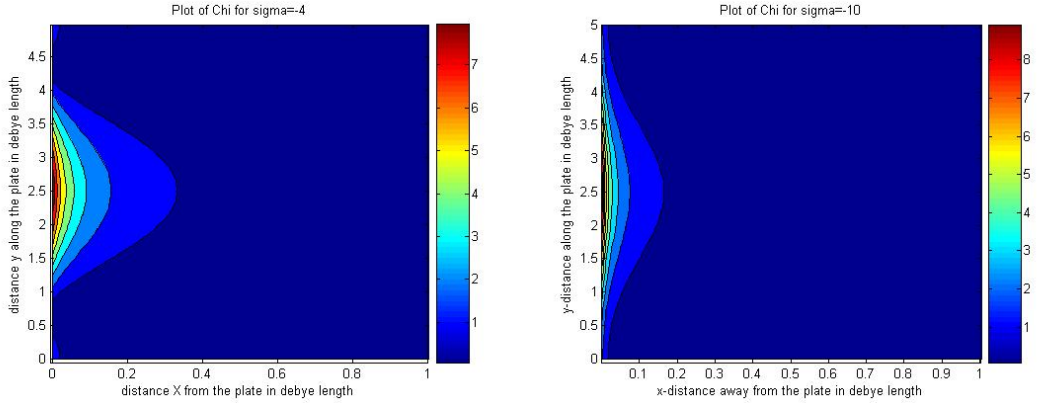

Figure 8: Plot of χ at very high surface charge densities. Note how the screening length decreases to less than 0.3 debye length. Variations at Y=λ_y /2 dominates.

The contour plots are pretty self explanatory. An important point to note is that the periodicity/wavelength of the fluctuating charge distribution is kept constant in all the plots above and all calculations are done for a fixed Debye length of 4.0311 angstroms.

It might seem counter-intuitive at first sight that the screening length decreases with charge density. One might expect that the higher the charge density, the more non-linear is the system and the farther away an ion needs to be before effects of the surface inhomogeneity are lost. However, it should be emphasized that the quantity plotted is the differential change in potential imposed by the fluctuating surface charge density and not the immediate impact of the surface charge on the potential. Therefore, as the surface charge density increases, the concentration of ions near the plate increases and screening of ions are readily available. Furthermore, effects of non linearity in the X-direction are so strong that they completely swamp out the weak variation of the surface charge in the y-direction. In fact this also explains how peaks at the “edges” of the plate get shorter and more diffused as the charge density increases. Except near the middle of the plate where surface charge density fluctuations are greatest, effects arising from the fluctuations in surface charges rapidly decays in importance near the “edges” of the plate with increased charge density.

On the other hand, for small charges where non-linearities in the y-direction are comparative to those in the x-direction, the effects of the surface charge fluctuations decay over a longer distance and retain most of its sinusoidal characteristics.

It was shown earlier that for long wavelength surface charge densities greater than -1 Cm^{-2}, the naïve approximation is simple, yet accurate in predicting the electrostatic potential. It can therefore be used in equations 5 and 6 to calculate the screening length analytically. Indeed, the results from the calculation are in good agreement with the numerical results and can be found in figure 9 on the following page. While similar calculations using the perturbative approximation agree with the numerical results qualitatively, the predicted screening lengths are approximately four times larger in magnitude. This is a consequence of the slower change in electrostatic potential observed in figure 5

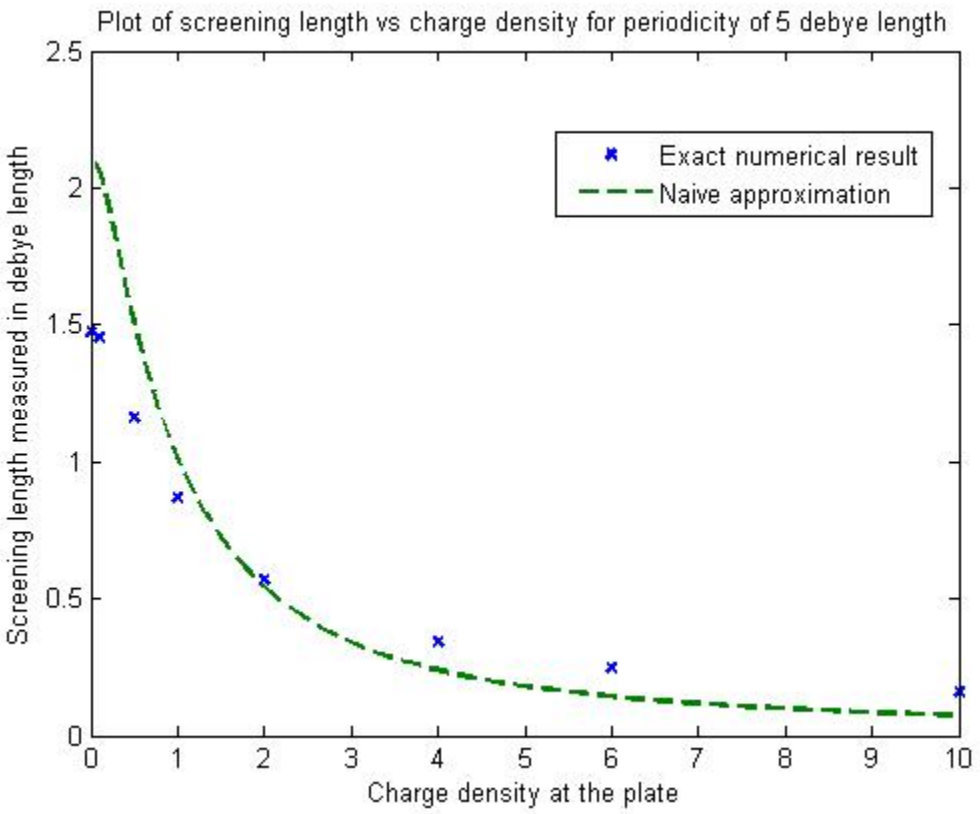

Figure 9: Comparison of naïve approximation to numerical calculation. The screening length approaches a constant value as charge density tends to infinity. Note also the better agreement at high charge densities.

5. Long wavelength vs. Short wavelength fluctuations

To account for short wavelength fluctuations, both the naïve and perturbative solutions cannot be used. As mentioned earlier, the good agreement between the naïve approximation and the numerical results occurs only when the ratio κ is small. As the wavelength of the fluctuations in the surface charge density decreases, the variations in the y direction can no longer be ignored and one cannot truncate the κ expansion to first order. In fact, it is easily seen that if one uses equation 2 or equation 4 to calculate the screening length, the result will be independent of the wavelength of fluctuations. In principle, expanding the perturbative solution to second order will provide us with the functional dependence of the screening length on λ_y. However, as described earlier, the second order perturbation solution leads to over correction and unphysical results.

Fortunately, in the other extreme situation when the wavelength is less than 1 debye length, fluctuations are so rapid that the electrolytes do not recognize the presence of surface inhomogeneity. It is observed that the screening length saturates to a constant value, L_{xo} of approximately 0.25 Debye length.

In the moderate wavelength regime, ($1<\lambda_y<4$) where fluctuations cannot be ignored, while the pertubative solution works slightly better than the naïve solution, it is clear that neither can be used. Unfortunately, I am unable to obtain any approximate solution that agrees with the numerical results. However, regression of the numerical results shows that the ratio of $\ln(\lambda_y)/(L_x-L_{xo})$ depends exponentially on the surface charge. As the charge density increases, L_x tends to L_{xo} and the ratio tends to infinity. Similarly, for a particular value of surface charge, the screening length L_x depends logarithmically on the length scale of the fluctuations in the y-direction. This is indeed consistent with the results obtained from the approximate solutions. The behavior in the intermediate regime is summarized in the figure 10 below:

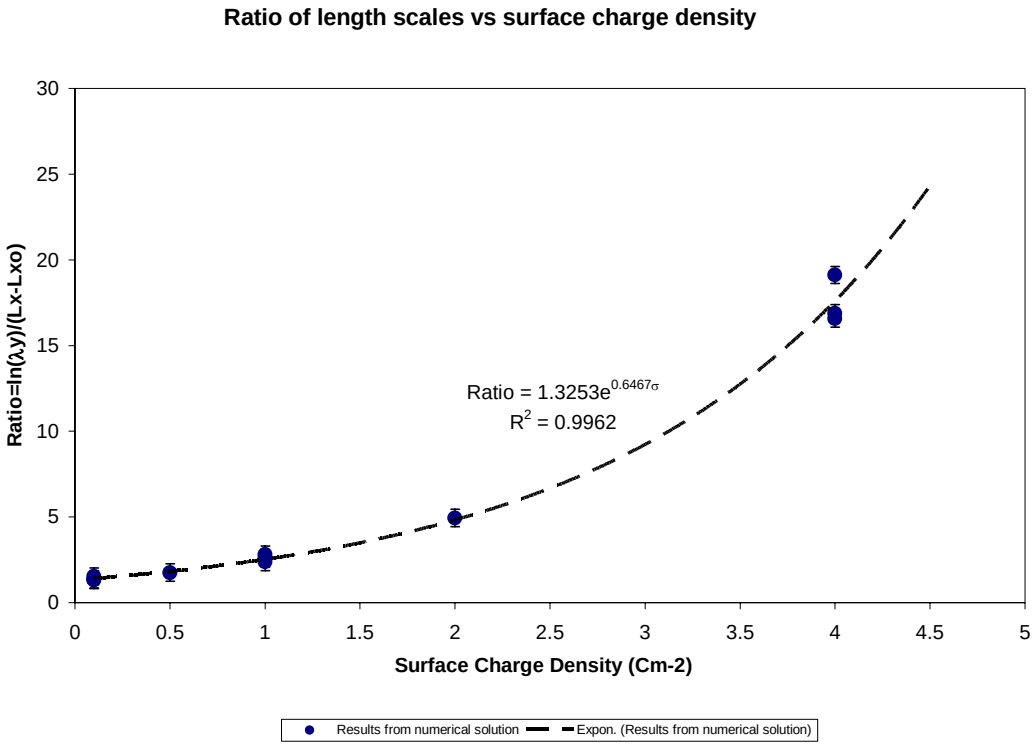

Figure 10: Numerical results for different surface charge and fluctuations are found to lie on a single curve characterized by the parameter $\ln(\lambda_y)/(L_x-L_{xo})$.

6. Conclusion

It is shown in this paper that perturbative and approximate solutions work well in the nonlinear regime where surface charges are high. The effects from the long wavelength fluctuations can be explained well with both perturbative and naive approximations when the ratio κ is small. Predictions of screening length are also in close agreement with numerical results.

In the other extreme, when the wavelength is less than 1 debye length, the screening length saturates to a constant value of approximately 0.25 debye length. In fact, the functional dependence of the screening length on the magnitude of the surface charge is best understood in terms of the competition of non-linear effects in the x and y direction. As surface charge increases, nonlinearities in the x-direction dominate and swamp out the effects of the fluctuations in the y-direction. This phenomenon is observed in both long and short wavelength fluctuations.

An analytical form of the solution is not available at moderate wavelength. However, it is found by regression that the ratio $\frac{\ln(\lambda_y)}{L_x - L_{xo}} \sim \exp(|\sigma|)$ relates the three variables to each other remarkably well. Interestingly, this ratio is also consistent with results from the high wavelength regime.

References

1. Heydweiller, Ann d. Physik (4) **33**, 145 (1910)
2. V.C. Wagner , Physikalische Zeitschrift **25** 474(1924)
3. L.Onsager, N.T. Samaras, J.Chem Phys **2**, 528 (1934)
4. J.K Percus, J Chem Phys, **75,** 1316, (1981)
5. W.Kunz, L.Belloni, O.Bernard, B.W Ninham, J Phys Chem B **108** (7): 2398 (2004)
6. J.M Barthel, H.Krienke, W.Kunz, Physical Chemistry of Electrolyte Solutions
7. E. Waisman, J.L Lebowitiz, J Chem Phys, **56**, 3086 (1972)
8. L. Teran, S.H Suh, H.S. White, H.T Davis, J Chem Phys. **92**, 5088, (1990)
9. Z.Tang, L. Teran, H.T Davis, Mol Phys. **71**, 369, (1990)
10. Z.Tang, L.E Scriven, H.T Davis, J Chem Phys. **97**, 494, (1992)

11. S. Nordholm, J.Gibson, M.A Hooper, J.Stat Phys **28**,391 (1982)

12. T. Vanderlick, H.T Davis, J.K Percus, J Chem Phys, **91**, 7136 (1989)

13. G.A Mansoori, N.F Carnahan, K.E Starling and T.W Leland, J Chem Phys, **54**, 1523 (1971)

14. R.R Netz and H Orland Eur. Phys Lett **45**(6), 726-732(1999)

15. R.R Netz and H Orland Eur. Phys J.E **1**,203-214(2000)

16. R.R Netz and H Orland Eur. Phys J.E **5**,557-574(2001)

17. R.R Netz and H Orland Eur. Phys J.E **11**, 301-311(2003)

18. P.Jungwirth, D. Tobias, J Phys Chem B **104** 7702 (2000)

19. D.Bhatt, J. Newman, C.J Radke, J. Phys Chem **108** (26) 9077-9084

20. W. Deen, Analysis of Transport Phenomena, Oxford University Press

Other works consulted:

21. L.Pauling, Proc.Royal Soc.A 114 (1927) 181

22. P.W.Atkins, Physical Chemistry, 5th ed, W.H.Freeman and Company, New York, 1994

23. J.M. Praunitz, R.N.Lichtenthaler, and E.G.de Azevedo, Molecular Thermodynamics of Fluid Phase Equilibra, Prentice-Hall, Englewood Cliffs, NJ, 1986

24. H.T. Davis, Statistical Mechanics of Phases, Interfaces and Thin Films. Wiley, 1997

25. J.S.Newman, Electrochemical Systems, 2nd ed.,Prentice-Hall,Englewood Cliffs, NJ, (1987)

Appendix A

1.Perturbative Solution to 2-D Poisson Boltzmann Equation

Zeroth order in κ:

$$\frac{\partial^2 \psi_o}{\partial X^2} = 2\sinh(\psi_o)$$

$$\left.\frac{\partial \psi_o}{\partial X}\right|_{x=0} = \frac{-ze\lambda_x\sigma}{4\sqrt{2}\varepsilon kT}$$

$$\psi_o(\infty) = 0$$

$$\Rightarrow \left[\frac{\partial \psi_o}{\partial X}\right]^2 = 4\cosh(\psi_o) + C_1 \qquad \Rightarrow \frac{\partial \psi_o}{\partial X} = \sqrt{4\cosh(\psi_o) + C}$$

$$Since \left.\frac{\partial \psi_o}{\partial X}\right|_{x=\infty} = \psi_o(\infty) = 0, \quad C_1 = -4 \Rightarrow \frac{\partial \psi_o}{\partial X} = 2\sqrt{\cosh(\psi_o) - 1} = -2\sqrt{2}\sinh\left(\frac{\psi_o}{2}\right)$$

Integrating wrt to ψ_o *and* X *:*

$$\Rightarrow tanh\left(\frac{\psi_o}{4}\right) = C_2 \exp\left(-\sqrt{2}X\right), \quad \text{however since at } X = 0, \psi_o(0) = 2\sinh^{-1}\left(\frac{ze\lambda_x\sigma}{4\sqrt{2}\varepsilon kT}\right),$$

$$C_2 = \tanh\left(\frac{1}{2}\sinh^{-1}\left(\frac{ze\lambda_x\sigma}{4\sqrt{2}\varepsilon kT}\right)\right) = \frac{-1+\sqrt{\left(\frac{ze\lambda_x\sigma}{4\sqrt{2}\varepsilon kT}\right)^2+1}}{\left(\frac{ze\lambda_x\sigma}{4\sqrt{2}\varepsilon kT}\right)} = \frac{2}{\sigma}\left[\sqrt{\sigma^2 + 8\rho\varepsilon kT} - \sqrt{8\rho\varepsilon kT}\right] = A$$

$$\Rightarrow \psi_o = 2\ln\left(\frac{1 + A\exp\left(-\sqrt{2}X\right)}{1 - A\exp\left(-\sqrt{2}X\right)}\right)$$

1st order in κ:

$$\frac{\partial^2 \psi_1}{\partial X^2} = 2\cosh(\psi_o)\psi_1(x,y)$$

$$\Rightarrow \frac{\partial^2 \psi_1}{\partial X^2} = \frac{2\left[1 + A^2 \exp\left(-2\sqrt{2}X\right)\right]}{1 - A^2 \exp\left(-2\sqrt{2}X\right)}\psi_1$$

$$\left.\frac{\partial \psi_1}{\partial X}\right|_{x=0} = \frac{-ze\lambda_y{}^2\sigma}{4\lambda_x\sqrt{2}\varepsilon kT}\eta\cos(Y)$$

$$\psi_1(\infty) = 0$$

$$\left.\frac{\partial \psi_1}{\partial Y}\right|_{Y=0} = 0$$

$$\left.\frac{\partial \psi_1}{\partial Y}\right|_{Y=\lambda_y} = 0$$

Let α *be* $1 - A^2 \exp\left(-2\sqrt{2}X\right)$

$$\Rightarrow [1-\alpha]^2 \alpha^2 \frac{\partial^2 \psi_1}{\partial \alpha^2} - [1-\alpha]\alpha^2 \frac{\partial \psi_1}{\partial \alpha} - \frac{1}{4}[2-\alpha]\psi_1 = 0$$

Assume that the solution can be expanded as $\sum_{k=0}^{\infty} a_k \alpha^{s+k}$ *and demanding that 1st term is not zero :*

It can be shown that :

$$s_{\pm} = \frac{1 \pm \sqrt{3}}{2},$$

$$a_1 = \frac{-2s^2 + 3s + 0.25}{0.5 - s^2 - s}\ a_o$$

for $k > 2$

$$a_k{}^{\pm} = \frac{0.25 + [k + s_{\pm} - 1][5 - 2k - 2s_{\pm}]a_{k-1} + [k + s_{\pm} - 2][k + s_{\pm} - 4]a_{k-2}}{[k + s_{\pm}][k + s_{\pm} - 1] - 0.5}$$

$$\Rightarrow \psi_1 = \sum_{k=0}^{\infty} a_k^{\pm}\left[1 - A^2 \exp\left(-2\sqrt{2}X\right)\right]^{k+s_{\pm}}$$

with $a_o^{\pm}$ *satisfying the boundary conditions.*

2.Exact Solution to the Linearized 2-D Poisson Boltzmann Equation

$$\frac{\partial^2\psi}{\partial X^2}+\frac{\partial^2\psi}{\partial Y^2}=2\psi(x,y)$$

Let $\phi_n(Y)=\sqrt{2}\cos(n\pi Y)$ *and* $\psi_n(X)=\int_0^{\lambda_y}\sqrt{2}\cos(n\pi Y)\psi(x,y)$ *for n = 0,1,2...*∞

$$\Rightarrow \frac{\partial^2\psi_n(X)}{\partial X^2}-(n\pi)^2\psi_n(X)=2\psi_n(X)$$

$$\left.\frac{\partial\psi_n}{\partial X}\right|_{x=0}=0 \text{ for } n\neq 0,2$$

$$\left.\frac{\partial\psi_n}{\partial X}\right|_{x=0}=\frac{-\lambda_x e\sigma\eta}{2\sqrt{2}\varepsilon kT} \text{ for } n=2$$

$$\left.\frac{\partial\psi_n}{\partial X}\right|_{x=0}=\frac{-\lambda_x e\sigma}{2\varepsilon kT} \text{ for } n=0$$

$$\psi_{n1}(\infty)=0$$

Solving for ψ_n *yeilds* :

$$\psi(x,y)=\frac{-\lambda_x e\sigma}{2\sqrt{2}\varepsilon kT}\left[\exp\left(-\sqrt{2}X\right)+\frac{\eta\cos(Y)}{\sqrt{2\pi^2+1}}\exp\left(-\sqrt{2+4\pi^2}X\right)\right]$$